*Desalination and Water Treatment*
www.deswater.com

doi: 10.1080/19443994.2013.768425

51 (2013) 5196–5203
July

Taylor & Francis
Taylor & Francis Group

# Preparation of ultrafiltration membrane by newly synthesized AMC polymer

In-Chul Kim[a,*], Yong-Sook Jin[a,b], Doo-Hyun Song[a], Su-Hyun Ahn[a,c], You-In Park[a]
Beom-Sik Kim[a], Jonggeon Jegal[a], Bong-Kuk Seo[a], Jong-Hak Kim[b], Young-Nam Kwon[d],
Chi-Joon Mo[e], Jeong-Jae Lee[e], Dong-Seong Kim[e], Seong-Han Lim[e]

[a]*Research Center for Biobased Chemistry, Korea Research Institute of Chemical Technology, P.O. Box 107,*
*Sinseongno 19, Yuseong, Daejeon 305-600, Republic of Korea*
*Email: ickim@krict.re.kr*
[b]*Department of Chemical and Biomolecular Engineering, Yonsei University, Seoul 120-749, Republic of Korea*
[c]*Department of Chemical and Biomolecular Engineering, Sogang University, Seoul 121-742, Republic of Korea*
[d]*School of Urban & Environmental Engineering, Ulsan National Institute of Science and Technology (UNIST),*
*Ulsan 689-798, Republic of Korea*
[e]*Manufacturing R&D Center, Hyosung, Anyang 431-080, Republic of Korea*

Received 15 June 2012; Accepted 28 September 2012

---

ABSTRACT

Water-soluble methyl cellulose was acetylated to use as a hydrophilic membrane material. The acetylation was preceded under mild conditions to keep a high molecular weight. Acetylation could be confirmed by Fourier transformation infrared spectroscopy (FT-IR). Acetylated methyl cellulose (AMC) membrane could be successfully fabricated by an immersion precipitation method. Various additives were added in a polymeric solution to control the pore size and cross-sectional structure. Using 1,4-dioxane and acetone as additives changed the membrane morphology from finger-like structure to sponge-like structure. A membrane fouling test was conducted by using protein bovine serum albumin (BSA). The membrane-fouling of the AMC membrane was compared with that of a polyvinylidene fluoride (PVDF) membrane. The AMC membrane showed much better fouling resistance against protein than the PVDF membrane.

*Keywords:* Metyl cellulose; Acetylation; Acetylated methyl cellulose; Fouling

---

## 1. Introduction

Ultrafiltration is a widely used process with many applications. Significant development of membrane separation technologies has been commercially achieved. These developments have been motivated by the needs in several industries to reduce the overall operational costs. Nevertheless, polymeric membranes are susceptible to fouling. Fouling worsens the membrane performance, shortens its life. The fouling results in the reduction in the flux and salt rejection. Surface hydrophobicity is considered as one of the major reasons for membrane fouling. It is generally accepted that fouling of polymeric membranes decreases with the

---

*Corresponding author.

*7th Aseanian Membrane Society Conference (AMS7), 4–7 July 2012, Busan, Korea*

increase in hydrophilicity of the polymeric materials. Cellulose acetate (CA) is a representative polymeric material to reduce the membrane fouling. However, the CA polymer has a low molecular weight and mechanical strength. A serious problem faced during the application of membrane filtration in water treatment is membrane fouling by various foulants like natural organic matter and protein. Membrane fouling can cause an increase in hydraulic resistance and a flux decline, increase operation and maintenance costs, and shorten the membrane life [1–4]. Ultrafiltration has the major variety of applications in different industries, because it is as a separation technology of high efficiency and low-energy consumption [5]. Currently, much effort has been devoted to improve the performance of the membranes in terms of antifouling properties, high mechanical strength, and good chemical resistance. CA membranes have low surface roughness and excellent hydrophilicity that is very important in minimizing fouling [6–10].

In this study, a cellulosic polymer was synthesized and a membrane was fabricated with the polymer. An acetylated methyl cellulose (AMC) membrane was fabricated by a phase inversion method. The membrane fouling of the AMC membrane was compared with that of polyvinylidene fluoride (PVDF) membrane.

## 2. Experimental

### 2.1. Materials

Pyridine and acetic anhydride (Sigma-Aldrich) were used for the acetylation of methyl cellulose (MC, Samsung fine chemical). AMC membrane was fabricated by a phase inversion method [11]. N,N-dimethyl acetamide (DMAc) was purchased from Samchun Chemical Industries. Polyvinylpyrrolidone (PVP, 30 K) and polyethylene glycol #600 (PEG600) were added in solution as an additive. These are purchased by Wako and Samchun Chemical Industries respectively. Acetone and 1,4-dioxane as a cosolvent were supplied by Burdick and Jackson and Junsei, respectively. Filtration solutions were prepared by dissolving polyethylene oxides (PEO) with molecular weights of 100,000, 200,000, and 600,000 from Sigma-Aldrich in deionized (DI) water. Bovine serum albumin (BSA, Sigma Aldrich) was selected as a foulant. DI water (Millipore, USA) was used as a coagulant in membrane preparation. All chemicals were used without further purification.

### 2.2. Synthesis of AMC

A mixture of 3 g of MC, 5 mL of pyridine, and 15 mL of acetic anhydride was stirred in a three-necked flask at 90˚C for 3 h under an atmosphere of nitrogen. Then, the mixture was poured into cold water to precipitate polymer, which was filtered and purified by repeated reprecipitation from water. The introduction of acetyl group by acetylation reaction was confirmed by Fourier transformation infrared spectroscopy (FT-IR). The chemical structure is shown in Fig. 1.

### 2.3. Preparation of AMC membranes

The AMC membranes were fabricated via the phase inversion process [6–10]. Basically, AMC was dissolved in DMAc at 100˚C under constant stirring

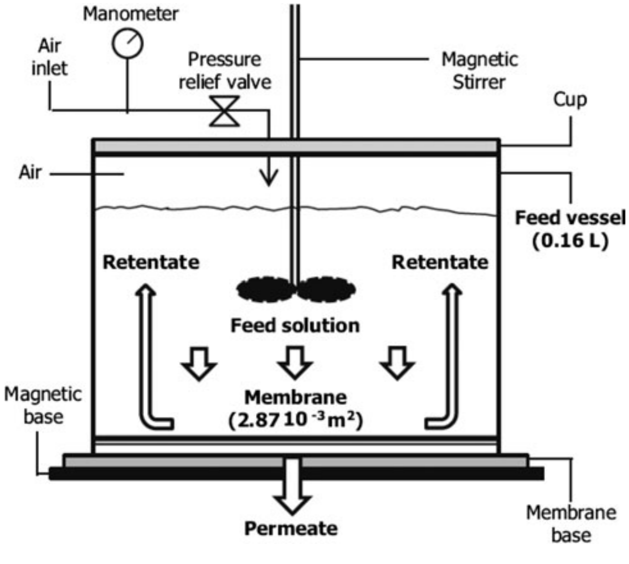

Fig. 2. Schematic diagram of the experimental UF unit.

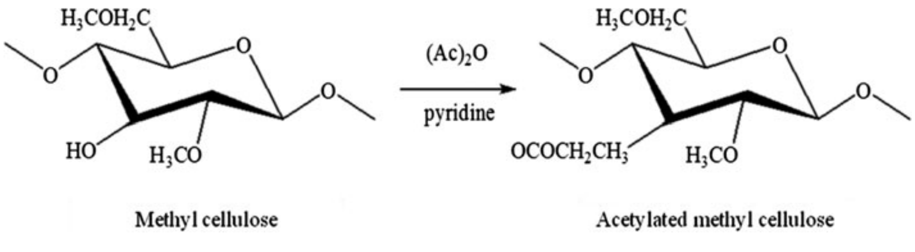

Fig. 1. Acetylation of methyl cellulose.

for at least 3 h until homogeneous solution was obtained. The casting solution was then degassed at 50˚C for another 1 h without stirring to allow complete release of bubbles. Afterward, the solution were cast on glass plate with a casting knife and the plates were subsequently immersed into a DI water bath with a temperature of 20˚C. The fabricated membranes were washed thoroughly with DI water to remove residual solvents and then kept in DI water before testing. The thickness of the wet membranes was about 250 μm.

### *2.4. Characterization of the AMC membranes*

The surface and cross-sectional morphology of the AMC membranes were studied using scanning electron microscope (SEM) (JSM-5610LVS, Japan) with an accelerating voltage of 15 kV. The membranes frozen in liquid nitrogen were broken and sputtered with gold before SEM analysis. A dead-end stirred cell filtration system connected with a nitrogen gas cylinder and solution reservoir was designed to characterize the performance of membranes. The system consists of a filtration cell (Model 8200, Millipore Co., USA) with a volume capacity of 200 mL and an inner diameter of 62 mm. The effective area of membrane was 28.26 cm$^2$. The feed side of system was pressed by nitrogen gas. All the filtration experiments were carried out at room temperature of 20˚C in a dead-end UF module of vertical flow as shown in Fig. 2. The cell was placed on a magnetic plate and the feed solution stirred by a magnetic bar in order to reduce concentration polarization. The membrane filter sheet was placed on the membrane base and the lowest part of the cell had been screwed together with the membrane and the base. The membranes were pressurized at 1 Kgf/cm$^2$ using DI water. The exposure time was 10 s. A rejection rate of the PEO was confirmed by HPLC. Membrane fouling test was conducted with the same apparatus. The aqueous BSA 100 ppm solution was used for the fouling test. Flux data were accumulated for 600 s. The operating pressure was 1 Kgf/cm$^2$. Atomic force microscope was used for the analysis of the membrane surface roughness.

## 3. Results and discussion

### *3.1. FT-IR analysis of AMC*

Characteristic FT-IR absorbance spectra have been used to determine the acetylation of MC as shown in Fig. 3. The MC exhibited the broad stretching vibration of hydroxyl group (–OH) about 3,500 cm$^{-1}$. Also upon the acetylation reaction between MC and acetic anhydride, a new strong characteristic peak appeared at 1,750 cm$^{-1}$, which is assigned to carbonyl group in AMC. The band at about 2,929 cm$^{-1}$ assigned to an asymmetric stretch vibration of CH$_2$ from the CH$_2$–OH group in MC. In addition, the shift of the stretching vibration of hydroxyl group (–OH) to a higher wave number attributed to the interaction between MC and acetic anhydride. As compare to MC, AMC shows the peak position of stretching vibration of CH$_2$ shift to higher wave number and this result came from coordinative interaction in acetylation. The results show that FT-IR spectroscopy can be used to assess the chemical structural changes in MC during acetylation reaction.

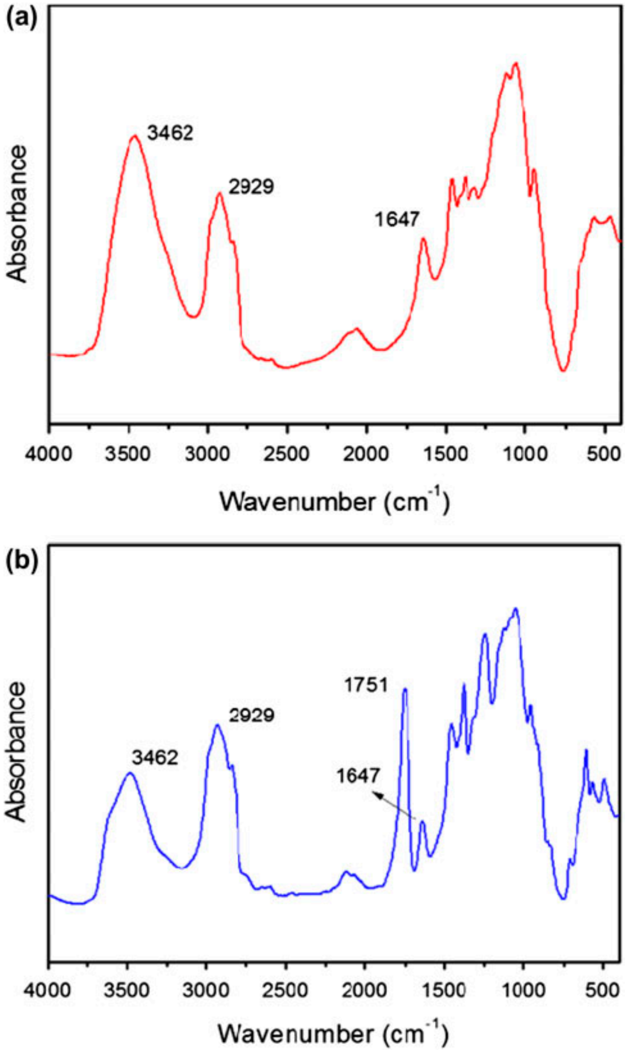

Fig. 3. FT-IR spectra of (a) methyl cellulose and (b) AMC.

### *3.2. Effect of AMC concentration on the properties of membrane*

AMC membranes were formed by non-solvent induced phase separation process. It is known that the

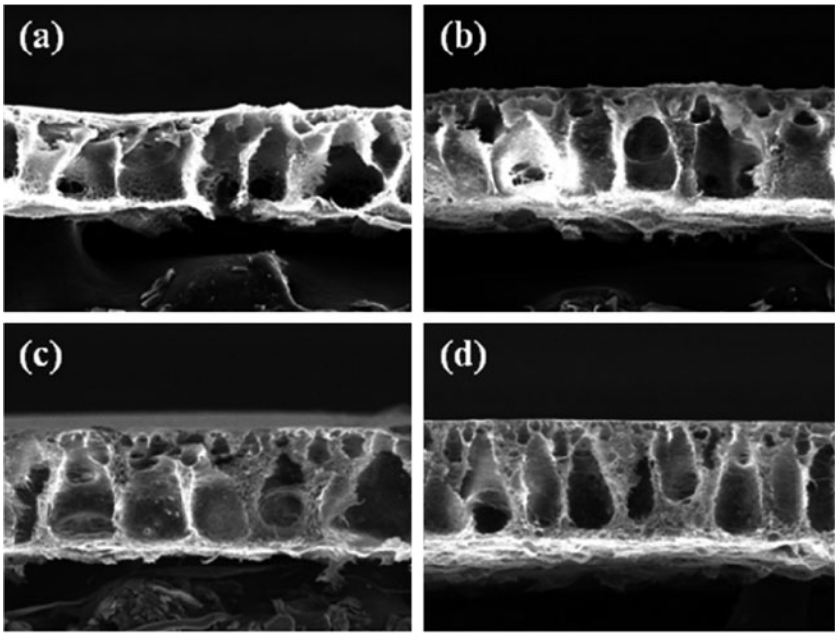

Fig. 4. Effect of AMC concentration on morphology of the synthesized flat sheet membrane; (a) AMC 7 wt% (b) AMC 10 wt% (c) AMC 12 wt% (d) AMC 14 wt%.

polymer concentration in the solution strongly influences the structure of the membrane. With 7, 10, 12, and 14 wt% AMC, respectively, were dissolved in DMAc at 100˚C added PVP 5 wt% as an additive under constant stirring for at least 5 h until homogeneous solution was obtained. The casting solutions were then degassed at 50˚C for another 1 h without stirring to allow complete release of bubbles. Afterward, the solutions were cast on glass plate with the help of baker film applicator. The cast membranes were evaporated for 10 s, followed by immersion in a bath containing water. The fabricated membranes were washed thoroughly with DI water to remove residual solvent and then kept in DI water before testing. The thickness of the wet membranes was about 250 μm. Four membranes were prepared by the same preparation method. Fig. 4 shows SEM images of membrane cross-sections. There is a noticeable variation in the membrane structure forming a finger-like morphology to a more densified structure for increasing AMC concentration. The pure water flux (PWF) and rejection of these membranes were plotted in Fig. 5. The rapid decrease in flux is observes. As can be observed, rejections of the synthesized membranes were reduced by increasing AMC concentration. Increasing AMC concentration from 7 to 14 wt% intensifies thermodynamic instability of the polymer solution, and thus, demixing of this concentrated solution can be performed with less amount of non-solvent.

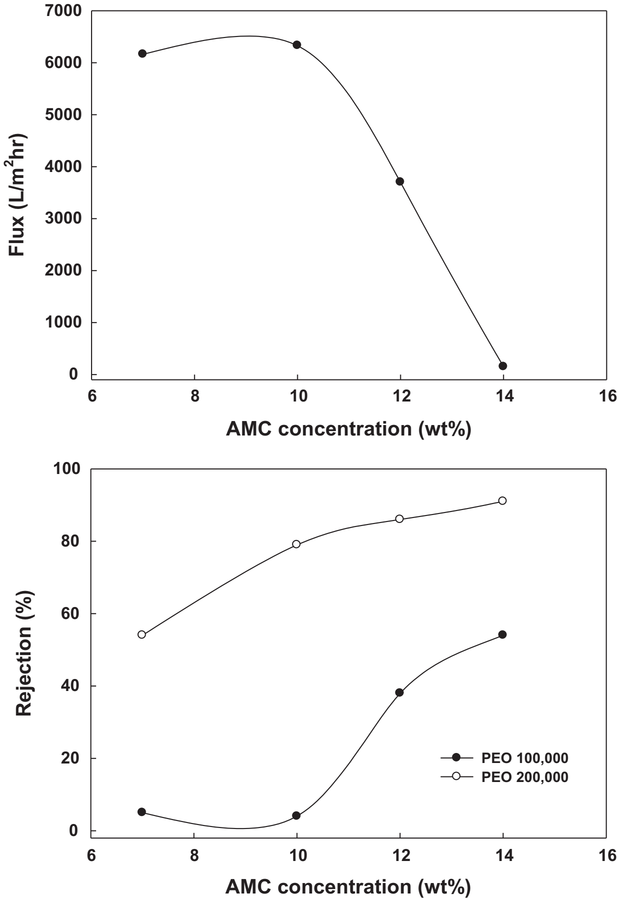

Fig. 5. Effect of AMC concentration on water flux and rejection.

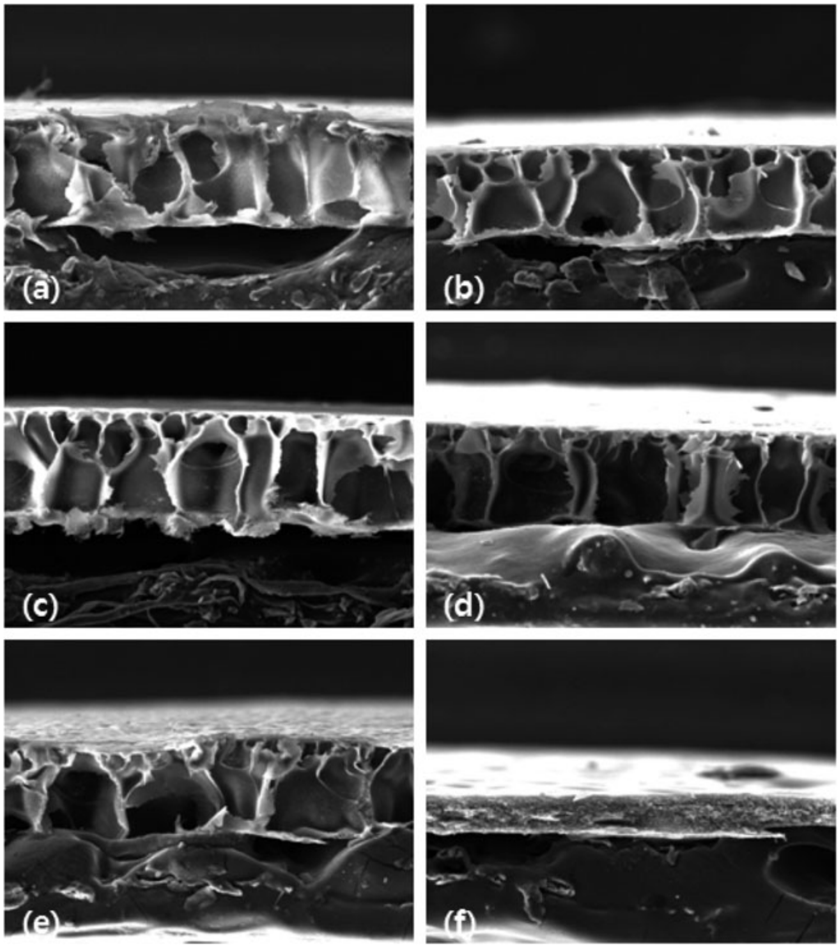

Fig. 6. Effect of 1,4-dioxane on morphology of AMC membranes; (a) D60 (b) D50 (c) D40 (d) D30 (e) D20 (f) D10.

### 3.3. *Effect of cosolvent composition*

CA is the acetate ester of cellulose, which is a famous hydrophilic membrane material. The concentrations of membrane material in the casting solutions were fixed at 10 wt% and added PEG600 5 wt% as an additive. 1,4-dioxane was used as a cosolvent in order to reduce the pore size of the membrane surface. The casting solutions of AMC and 1,4-dioxane in DMAc were homogenous without observable phase separation. The volume content of 1,4-dioxane in solvent is 75, 65, 55, 45, 35, and 25, respectively, named as D10, D20, D30, D40, D50, and D60.

Fig. 6 shows the SEM images of the membrane morphology. These membranes had similar finger-like structures except for D10. D10 membrane shows completely sponge-like structure. In other words, no macrovoids were shown. The specific results are shown in Table 1. It is confirmed that cross-section structure was dense as 1,4-dioxane content increased over 75 wt% like D10. AMC membranes with DMAc have remarkably higher PWFs. Fig. 7 shows the PWFs of the prepared AMC membranes increased from 152 to 1,328 L/m$^2$h with an increase in DMAc content from 10 to 60 wt%. Moreover, by increasing the amount of 1,4-dioxane in the casting solution, macrovoids were disappeared due to the delayed demixing. In general, cosolvent can increase the solvent power,

Table 1
Effect of 1,4-dioxane on membrane performance

| Membrane | 1,4-dioxane | PWF (LMH) | *R*(%) of PEO 100,000 | *R*(%) of PEO 200,000 |
|---|---|---|---|---|
| D10 | 75 | 152 | – | – |
| D20 | 65 | 373 | – | – |
| D30 | 55 | 449 | 54 | 79 |
| D40 | 45 | 665 | 65 | 84 |
| D50 | 35 | 804 | 63 | 80 |
| D60 | 25 | 1,328 | 52 | 75 |

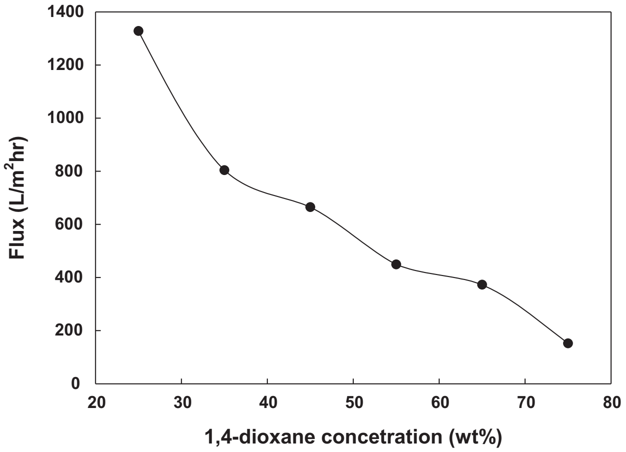

Fig. 7. Effect of 1,4-dioxane on water flux.

which means that the cosolvent can easily break interaction force between polymeric chains. In other words, the intrusion rate of non-solvent through the polymeric solution can be slow. For delayed demixing, more compact skin layer can be formed due to the inhibition of the inflow of non-solvent into the polymeric solution. In the case of delayed demixing, the introduction of the nuclei of polymer-poor phase would be delayed. Therefore, macrovoids are significantly disappeared. Without the addition of 1,4-dioxane, large macrovoids were shown due to the instantaneous demixing, which means that the inflow rate of non-solvent becomes much faster than the outflow rate of solvent mixture. The instantaneous demixing results in more porous structure of the upper part of the membrane.

As shown in Table 1, the rejection of D40 membrane was 84%, which means that majority of PEO 200,000 could not go through the D40 membrane. The concentration polarization layer was easily formed in this case [12–15].

Introduction good solvent in the AMC casting solution lets the macrovoids appear at the membrane

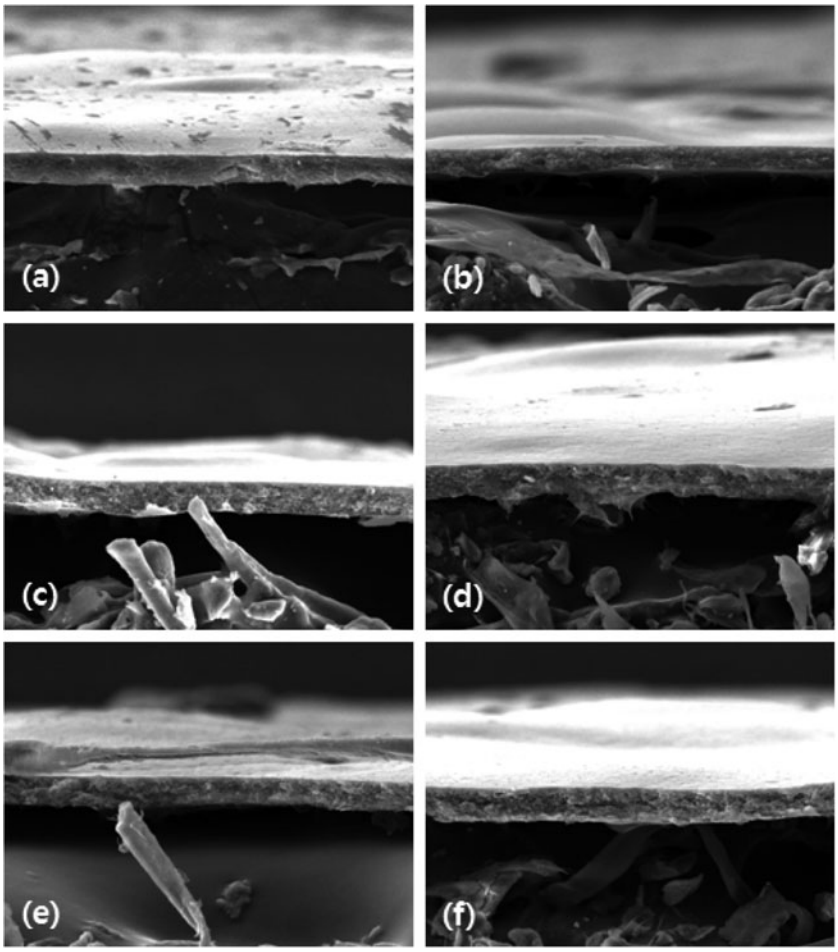

Fig. 8. Effect of 1,4-dioxane and acetone concentration on morphology of AMC membranes (1,4-dioxane/acetone); (a) 1:4 (b) 1:3 (c) 1:2 (d) 1:1 (e) 2:1 (f) 3:1.

Table 2
Membrane performance used for protein-fouling test

| Membrane | PWF (LMH) | MWCO |
|---|---|---|
| AMC | 2,100 | PEO 200,000 |
| PVDF | 1,900 | PEO 200,000 |

cross-section. Instead of good solvent of DMAc, solvent mixture of acetone and 1,4-dioxane was used. Homogeneous casting solution could be obtained. From the cross-section images of Fig. 8, it can be observed that the membranes showed sponge-like structures at the membrane cross-section. It can be explained that acetone which has a low boiling point can evaporate at the membrane surface during solution casting, which means that the polymer concentration of the membrane surface until the nascent membrane is immersed into the coagulant becomes higher. The synergy effect of 1,4-dioxane and acetone on the demixing process can supply more compact surface and sponge-like structure at the membrane cross-section.

### 3.4. Improvement in antifouling property

The surface roughness is an important factor affecting the antifouling property of membrane. The flux change could be explained by the balance between the pore-covering effect and the increase in surface roughness. It is generally accepted that improvement in the hydrophilicity and surface roughness of microporous membrane may bring some increase in the water permeation flux. The main factor inducing the protein fouling was thought to be the interaction between the protein and the membrane [16]. In general, protein cannot attach on more smooth and hydrophilic membrane surface.

Before fouling test, the AMC and PVDF membranes with similar membrane performance were fabricated. Table 2 shows the results. Two membranes have similar water flux and the same pore sizes.

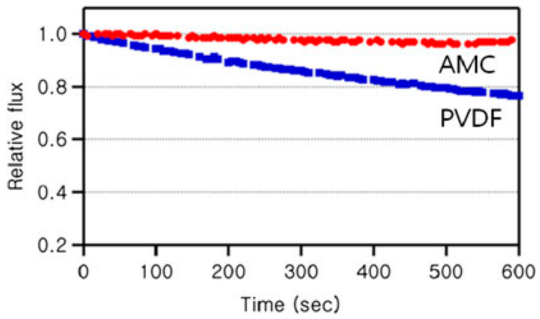

Fig. 9. Protein fouling of the AMC membrane.

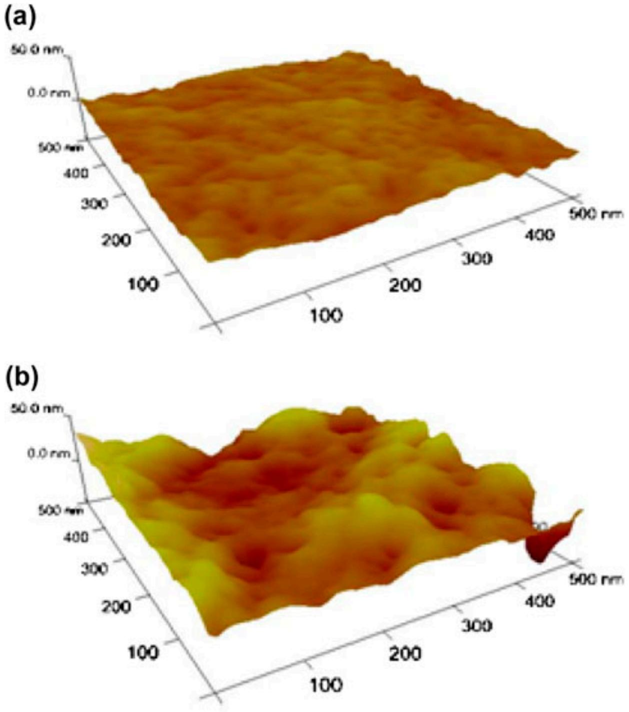

Fig. 10. AFM images of (a) AMC and (b) PVDF membrane.

Fig. 9 shows that the AMC membrane has much better fouling resistance against protein than the PVDF membrane. The flux decline of the AMC membrane is not shown. In contrast, the flux decline of the PVDF membrane is very fast. Fig. 10 shows the surface roughness of the AMC and PVDF membrane. The surface of the AMC membrane is very smooth. However, the surface of the PVDF membrane is very rough. These results can explain the reason of the low fouling of the AMC membrane.

## 4. Conclusions

AMC could be successfully prepared by acetylation of MC. The effect of additives on the AMC membrane performance was investigated. Membrane morphologies were observed by SEM. Increasing 1,4-dioxane concentration in the casting solution resulted in a decrease in flux and an increase in PEO rejection. Macrovoids in the membrane cross-section were completely disappeared by using 1,4-dioxane as an additive. The correlation between membrane surface morphology and fouling property was investigated by the filtration of BSA solution. The slow decline in the relative flux was shown in case of AMC membrane. In contrast, more significant flux decline was observed in the PVDF membrane. AMC membrane still showed higher antifouling effect compared with PVDF membranes due to smooth surface. Thus, membrane roughness is quite important for achieving useful anti-fouling property as well as a lower decrease in water permeability during filtration.

## References

[1] M. Pontie, A. Thekkedath, K. Kecili, H. Habarou, H. Suty, J.P. Croue, Membrane autopsy as a sustainable management of fouling phenomena occurring in MF, UF and UF processes, Desalination 204 (2007) 155–169.

[2] A.W. Zularisam, A.F. Ismail, M.R. Salim, M. Sakinah, H. Ozaki, The effects of natural organic matter (NOM) fractions on fouling characteristics and flux recovery of ultrafiltration membranes, Desalination 212 (2007) 191–208.

[3] E.M. Vrijenhoek, S. Hong, M. Elimelech, Influence of membrane surface properties on initial rate of colloidal fouling of reverse osmosis and nanofiltration membranes, J. Membr. Sci. 188 (2001) 115–128.

[4] Q. Shi, Y. Su, S. Zhu, C. Li, Y. Zhao, Z. Jiang, A facile method for synthesis of pegylated polyethersulfone and its application in fabrication of antifouling ultrafiltration membrane, J. Membr. Sci. 303 (2007) 204–212.

[5] F. Liu, N.A. Hashimi, Y. LiuPhillip, M.R.M. Abed, K. Li, Progress in the production and modification of PVDF membranes, J. Membr. Sci. 375 (2011) 1.

[6] Jian-Jun Qin, Maung Htun Oo, Yi-Ming Cao, Leng-Siang Lee, Development of a LCST membrane forming system for cellulose acetate ultrafiltration hollow fiber, Sep. Purif. Technol. 42 (2005) 291–295.

[7] Yiming Zeng, Zhigang Wang, Lijun Wan, Yanqiao Shi, Guanwen Chen, Chunli Bai, Surface morphology and nodule formation mechanism of cellulose acetate membranes by atomic force microscopy, J. Appl. Polym. Sci. 88 (2003) 1328–1335.

[8] R. Malaisamy, R. Mahendran, D. Mohan, Cellulose acetate and sulfonated polysulfone blend ultrafiltration membranes. II. Pore statistics, molecular weight cutoff, and morphological studies, J. Appl. Polym. Sci. 84 (2002) 430–444.

[9] Ani Idris, Lee Kuan Yet, The effect of different molecular weight PEG additives on cellulose acetate asymmetric dialysis membrane performance, J. Membr. Sci. 280 (2006) 920–927.

[10] Yen-Ning Kuo, Juan Hong, A new method for cellulose membrane fabrication and the determination of its characteristics, J. Colloid Interf. Sci. 285 (2005) 232–238.

[11] M. Mulder, Basic Principles of Membrane Technology, Kluwer Academic Publishers, Dordrecht, 1996.

[12] K.J. Hwang, T.T. Lin, Effect of morphology of polymeric membrane on the performance of cross-flow microfiltration, J. Membr. Sci. 199 (2002) 41–52.

[13] A.I. Schafer, A.G. Fane, T.D. Waite, Fouling effects on rejection in the membrane filtration of natural waters, Desalination 131 (2000) 215–224.

[14] A.I. Schafer, U. Schwicker, M.M. Fischer, A.G. Fane, T.D. Waite, Microfiltration of colloids natural organic matter, J. Membr. Sci. 171 (2000) 151–172.

[15] Q. Gan, Evaluation of solids reduction and backflush technique in crossflow microfiltration of a primary sewage effluent, Resour. Conserv. Recy. 27 (1999) 9–14.

[16] G. Belfort, R.H. Davis, A.L. Zydney, The behavior of suspensions and macromolecular solutions in crossflow microfiltration, J. Membr. Sci. 96 (1994) 1–58.